Cell, Vol. 106, 275–286, August 10, 2001, Copyright ©2001 by Cell Press

Telomere Dysfunction Increases Mutation Rate and Genomic Instability

Jennifer A. Hackett,[1] David M. Feldser,[1] and Carol W. Greider[2,3]

[1] Predoctoral Training Program in Human Genetics and Molecular Biology

[2] Department of Molecular Biology and Genetics
Johns Hopkins University School of Medicine
Baltimore, Maryland 21205

Summary

The increased tumor incidence in telomerase null mice suggests that telomere dysfunction induces genetic instability. To test this directly, we examined mutation rate in the absence of telomerase in *S. cerevisiae*. The mutation rate in the *CAN1* gene increased 10- to 100-fold in *est1*Δ strains as telomeres became dysfunctional. This increased mutation rate resulted from an increased frequency of terminal deletions. Chromosome fusions were recovered from *est1*Δ strains, suggesting that the terminal deletions may occur by a breakage-fusion-bridge type mechanism. At one locus, chromosomes with terminal deletions gained a new telomere through a Rad52p-dependent, Rad51p-independent process consistent with break-induced replication. At a second locus, more complicated rearrangements involving multiple chromosomes were seen. These data suggest that telomerase can inhibit chromosomal instability.

Introduction

Tumorigenesis involves the accumulation of genetic changes by the induction of a mutagenic process (Loeb, 1991). Two major classes of genetic instability have been characterized: microsatellite instability and chromosomal instability (reviewed in Lengauer et al., 1998; Cahill et al., 1999). Chromosomal instability is present in most solid tumors and begins at a very early stage of tumorigenesis (Shih et al., 2001). It includes both karyotypic changes and losses of heterozygosity (LOH). LOH frequently involves interchromosomal rearrangements, such as nonreciprocal translocations (Thiagalingam et al., 2001).

An increased cancer incidence in late generation $mTR^{-/-}$ telomerase null mice implicated telomere dysfunction as a factor that can contribute to tumorigenesis (Blasco et al., 1997; Rudolph et al., 1999). The frequency of tumor formation in $mTR^{-/-}$ mice is enhanced by p53 deficiency, possibly because the lack of a response to DNA damage allows increased genetic instability (Chin et al., 1999; Artandi et al., 2000). In late generation $mTR^{-/-}$ $p53^{-/-}$ tumors, the frequencies of chromosome fusions, anaphase bridges, and nonreciprocal translocations increase, suggesting that telomere dysfunction may initiate chromosomal instability (Chin et al., 1999; Artandi et al., 2000).

Telomeres are required for the stable transmission of linear chromosomes, and they distinguish natural DNA ends from DNA breaks that can participate in chromosomal rearrangements (Muller, 1938; McClintock, 1941). Telomere function is conferred both by the DNA sequence and by the proteins that bind to telomeres. In the yeast *S. cerevisiae*, telomeres consist of ~300 base pairs of TG_{1-3} repeats (Zakian, 1989) that are elongated by the ribonucleoprotein enzyme, telomerase (Greider and Blackburn, 1985; Singer and Gottschling, 1994). In vivo elongation of telomeres by telomerase requires four protein components (Est1p, Est2p, Est3p, Cdc13p) (Lundblad and Szostak, 1989; Lendvay et al., 1996) and one RNA component (*Tlc1*) (Singer and Gottschling, 1994). Mutations in any of these five genes result in telomere shortening and loss of cell growth capacity (Lendvay et al., 1996). Telomere maintenance also requires telomere binding proteins, including a negative regulator of telomere length, Rap1p, and, surprisingly, the nonhomologous end-joining (NHEJ) proteins Yku70p, Yku80p, Rad50p, Mre11p, and Xrs2p (reviewed in Gasser, 2000).

Disruption of telomere maintenance is associated with end-to-end chromosome fusion in many organisms. In the fission yeast *S. pombe*, deletion of the telomerase reverse transcriptase (trt^+) gene or both ATM homologs ($tel1^+$ and $rad3^+$) causes telomere shortening and eventual loss of growth. The few cells that escape growth arrest have circularized all three of their chromosomes (Naito et al., 1998; Nakamura et al., 1998). In *K. lactis*, mutations in the template region of telomerase RNA that alter the Rap1p binding site lead to circularization of chromosomes with retention of telomere sequence at the fusion junction (McEachern et al., 2000). No direct evidence of end-to-end chromosome fusions as a result of telomere dysfunction has been reported for *S. cerevisiae*.

End-to-end chromosome fusions can produce dicentric chromosomes. The two centromeres are frequently pulled to opposite spindle poles during mitosis, creating an anaphase bridge which is resolved by chromosome loss or a chromosome break which may involve loss of essential genes (McClintock, 1941; Haber et al., 1984). The resulting broken ends can undergo subsequent fusions, perpetuating a breakage-fusion-bridge (BFB) cycle (McClintock, 1941).

To directly determine whether telomere dysfunction can induce genetic instability, we measured the *CAN1* mutation rate in *est1*Δ yeast. We show that telomere dysfunction is associated with an increase in mutation rate. This increased mutation rate is caused by an increased frequency of gross chromosomal rearrangements involving terminal deletions that can cause nonreciprocal translocations. End-to-end chromosome fusion junctions have been isolated from yeast with short telomeres, indicating that BFB is one mechanism for the creation of terminal deletions.

Results

Telomere Shortening Increases the Mutation Rate

To investigate the effect of telomere shortening on genetic instability, the mutation rate of the *CAN1* gene was

[3] Correspondence: cgreider@jhmi.edu

measured in *est1*Δ yeast that show progressive telomere shortening (Lundblad and Szostak, 1989). Cells containing mutations in *CAN1*, which encodes an arginine permease, can be selected by plating on media lacking arginine, but containing the toxic arginine analog canavanine (Whelan et al., 1979). *CAN1* may be inactivated by point mutations or by chromosomal rearrangements that result in deletion of the locus (Chen et al., 1998).

As telomeres shorten in yeast, the growth rate of the population decreases after a lag period (Singer and Gottschling, 1994; Lendvay et al., 1996). When the growth rate is low, survivors emerge that have elongated their telomeres via a recombinational pathway (Lundblad and Blackburn, 1993). Because *est1*Δ cells with short telomeres have a decreased growth rate, we reintroduced *EST1* expression behind the *GAL1* promoter. The reintroduction of Est1p restored growth potential so that cells could form colonies. *GAL/EST1* expression was repressed in liquid culture but induced upon plating. *est1*Δ strains grown with or without the *GAL/EST1* vector had indistinguishable growth characteristics when grown in repressing conditions (data not shown). Reintroduction of *EST1* expression prevented a decrease in colony number and size when *est1*Δ cells were plated (data not shown). The *GAL/EST1* vector was included in all assayed strains, including the wild-type controls.

To assay the change in the fraction of growing cells in specific strains, ten parallel cultures were grown in continuous log phase for 11 days (Figure 1A). Each day, samples were plated onto canavanine plates to measure the mutation rate. The wild-type *CAN1* mutation rate was constant at about 1×10^{-7} over the course of the experiment (Figure 1B), consistent with previous measurements (Marsischky et al., 1996). Early in the growth curve (days 3–6), the mutation rate in the *est1*Δ strain was indistinguishable from wild-type. However, at the low point of the growth curve (day 7–8), the mutation rate in *est1*Δ cells increased about 10-fold over wild-type levels to 1×10^{-6}. After the generation of survivors in *est1*Δ cultures, the mutation rate returned to a level similar to wild-type cells (days 9–11).

The Increase in Mutation Rate in *est1*Δ Strains Is Associated with an Increased Frequency of Chromosomal Rearrangements

To determine what types of mutations occurred during the period of increased mutation rate, canavanine-resistant (can^R) colonies were assayed for the presence of the *CAN1* locus by colony PCR. The frequency of *CAN1* deletion was nearly identical in wild-type and *est1*Δ cultures early in the growth curve (day 4) (Figure 1C). However, on day 7, the frequency of deletion had increased in *est1*Δ cultures to about 10 times that of wild-type cultures, suggesting that gross chromosomal changes caused the increase in mutation rate.

To further characterize the changes in these *CAN1*-deleted colonies, the chromosome containing *CAN1* (chromosome V) was analyzed by pulsed field gel electrophoresis. A probe from within the most telomeric essential gene, *PCM1,* was hybridized to pulsed field gels resolving either whole chromosomes (Figure 1E) or NotI restriction fragments (Figure 1F). For all control canavanine-sensitive (CAN^S) colonies (lanes 1–4, 24–27), the *PCM1* probe hybridized to the correct 47.9 kb NotI fragment and to chromosome V in whole chromosome gels. *CAN1*-deleted cells from wild-type controls (lanes 5–9) had either a truncated chromosome V or a rearrangement involving chromosome V and one other chromosome. All *est1*Δ *CAN1*-deleted colonies (lanes 10–23) had chromosomal rearrangements, many of which produced *PCM1* hybridization on multiple chromosomes and multiple NotI fragments. Colonies with multiple bands were replated to single colonies. Pulsed field gel analysis of these colonies showed that the different bands were present in different cells in the original colonies (data not shown). Some *est1*Δ colonies (lanes 11, 13, 15, 17) had very faint hybridization of the probe to whole chromosomes, but showed similar loading of DNA (Figure 1D) and contained a single prominent band when the DNA was digested with NotI (Figure 1F). These samples had high levels of hybridization to the DNA in the wells in the uncut samples, suggesting that *PCM1* might be located on a circular chromosome that is unable to migrate out of the well.

Telomere Shortening Produces Terminal Deletions

To investigate the formation of the chromosome rearrangements, strains were constructed in which there were no essential genes near the reporter gene. At its native locus, *CAN1* is only 10 kb from *PCM1*. Thus, *CAN1* was moved to a location near the telomere on the left arm of chromosome XV, 43 kb from the most telomeric essential gene *DCP1* (TELO strain) (Figure 2A). The *ADE2* gene was placed just telomeric to *CAN1* so that canavanine-resistant cells with point mutations or small deletions in *CAN1* would produce white colonies, while deletions of a large chromosomal region including both *CAN1* and *ADE2* would produce red colonies. A second strain was constructed, in which the same construct containing *ADE2* and *CAN1* was placed centromeric to *DCP1* (After Essential or AE strain) (Figure 2A).

The *est1*Δ TELO and AE strains showed a similar decline in growth rate from day 3–8 (Figure 2B). The white colony *CAN1* mutation rates for wild-type and *est1*Δ cells from both the TELO and AE strains were similar to each other and were constant throughout the experiment (Figure 2C). Therefore, there is no increase in the rate of formation of point mutations or small deletions when telomeres are short. In contrast, the red colony *CAN1* mutation rate, representing large deletions, increased to 50-fold higher than wild-type in the *est1*Δ TELO strain at day 8 when the fraction of dividing cells was low. However, in the AE strain, the red colony mutation rate in *est1*Δ strains was constant throughout the experiment and identical to the wild-type rate (Figure 2C), indicating that telomere dysfunction induces terminal, but not internal, deletions.

Terminal Deletions in the TELO Strain Are Frequently Healed by Break-Induced Replication

To look directly at chromosomal changes in *CAN1* mutants, chromosomes were digested with PmeI, which cuts 93.5 kb from the left telomere of chromosome XV in the TELO strain (Figure 2A). Almost all wild-type and *est1*Δ *ade2can1* colonies from the TELO strain had terminal PmeI fragments that were shorter than the wild-

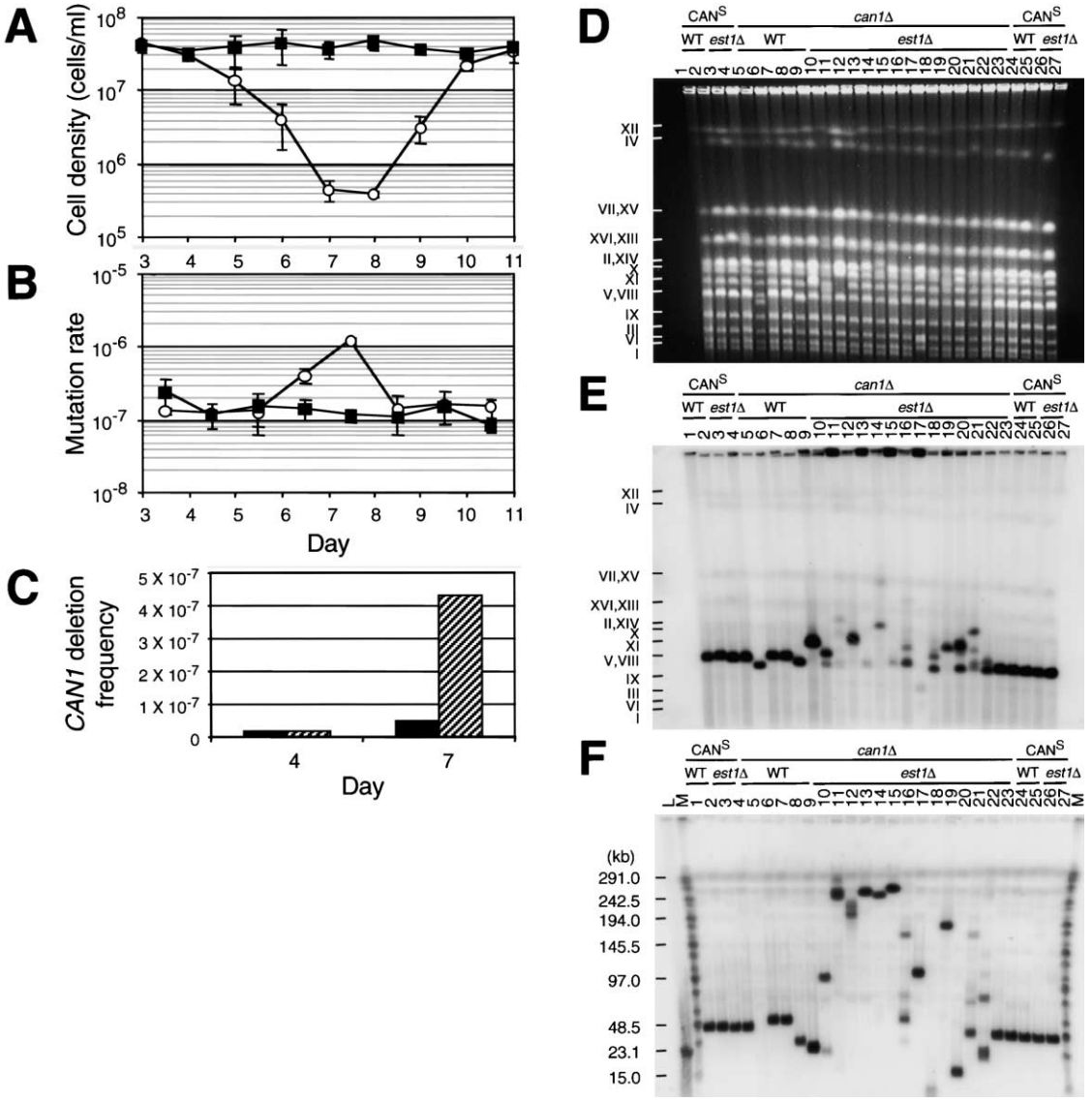

Figure 1. The *CAN1* Mutation Rate at the Native Locus Increases in *est1*Δ Strains

(A) Wild-type and *est1*Δ growth fraction averaged for 3 independent experiments. The plotted cell density is: (final concentration × (1×10^4 cells/ml) / initial concentration). Black squares: wild-type; open circles: *est1*Δ.

(B) Mutation rate averaged from 3 independent experiments. The mutation rate calculated from cells plated on a given day is plotted between that day and the previous day because it reflects the mutation rate as the cells grew from one day to the next. Black squares: wild-type; open circles: *est1*Δ.

(C) Frequency of deletion of the *CAN1* locus determined by PCR. Black bars: wild-type; hatched bars: *est1*Δ.

(D) Ethidium bromide-stained pulsed field gel resolving whole chromosomes. This gel was probed in (E).

(E) Pulsed field gel of whole chromosomes from wild-type and *est1*Δ control (CAN^S) and mutant (*can1*Δ) colonies probed with sequence from the essential gene *PCM1* on chromosome V.

(F) Pulsed field gel of NotI-digested chromosomes probed with *PCM1*. The wild-type terminal NotI fragment length is 47.9 kb. *CAN1* is located at 31.7–33.5 kb. *PCM1* is located at 43.3–44.9 kb. L: λ DNA/HindIII fragments; M: MidRange PFG marker I (NEB). DNA samples are identical to those in (E). The hybridizing band in lane 5 ran off the gel (6.8 kb).

type length (Figures 3B–3D). If a break that occurred between *CAN1* and *DCP1* had been repaired by de novo telomere addition when the cells were plated on galactose and *EST1* was expressed, it would have resulted in terminal restriction fragment lengths ranging from 10 to 54 kb shorter than wild-type. However, the recovered fragment lengths were all between 5 and 25 kb shorter than wild-type. Strikingly, multiple colonies had fragments with the same length, even when derived from independent cultures. These clustered fragment lengths suggested that broken chromosomes were healed by a mechanism that would result in the addition of defined amounts of sequence to the end of the broken chromosome, such as break-induced replication (BIR) (Malkova et al., 1996; Bosco and Haber, 1998) or telomere addition using a set of preferred addition sites (Kramer and Ha-

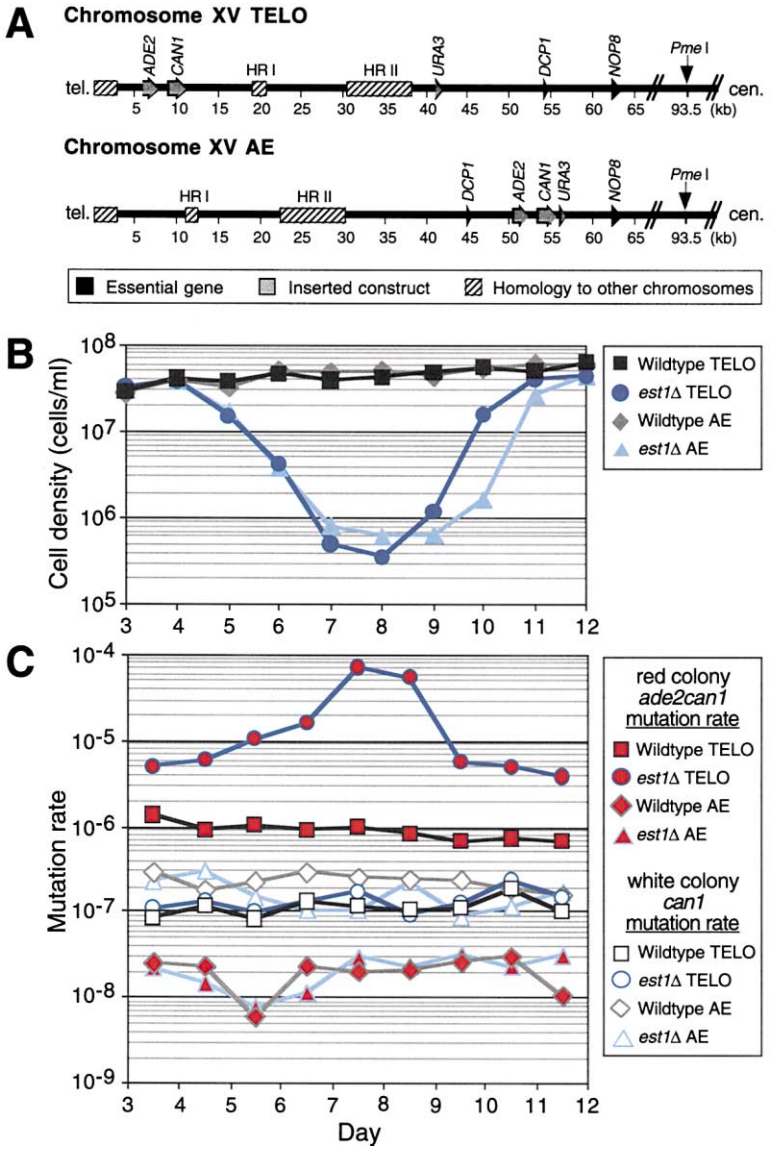

Figure 2. Telomere Dysfunction Increases the Deletion Mutation Rate at Sites Telomeric to Essential Genes

(A) Diagrams of engineered left arm of chromosome XV from the TELO (*telo*meric) and AE (After Essential) strains. Essential genes: black arrows; inserted genes: gray arrows; regions of sequence similarity to other chromosomes: hatched boxes; terminal PmeI restriction enzyme cut sites: vertical arrows. TELO: *ADE2* and *CAN1* were inserted near the telomere. *URA3* was inserted centromeric to the two regions of sequence similarity with other chromosomes, HRI and HRII. AE: *ADE2*, *CAN1*, and *URA3* were inserted centromeric to the most telomeric essential gene *DCP1*.

(B) Growth fraction for wild-type and *est1*Δ TELO and AE strains. TELO strain curves are the average of 2 experiments. Black squares: wild-type TELO; dark blue circles: *est1*Δ TELO; gray diamonds: wild-type AE; light blue triangles: *est1*Δ AE.

(C) Mutation rate for wild-type and *est1*Δ TELO and AE strains. TELO strain mutation rates are the average of 2 experiments. Symbols correspond to those in B. Red centers indicate the red colony (*ade2can1*) mutation rate. White centers indicate the white colony (*can1*) mutation rate.

ber, 1993). BIR involves a broken end invading another chromosome at a region of homology and initiating copying of the intact chromosome onto the end of the broken chromosome. Chromosome XV has two regions near the left telomere that are highly homologous to regions near telomeres on other chromosomes (HRI and HRII) (Figure 2A). Fifteen chromosome arms share 439–1744 bp of sequence with HRI with 89%–96% identity. Six chromosome arms share 516–7704 bp of sequence with HRII with 85%–97% identity. Repair of a break in chromosome XV through BIR using one of these regions of homology to initiate the copying of terminal sequence would produce terminal PmeI restriction fragments 5–30 kb shorter than the wild-type chromosome (Figure 3A), consistent with the observed wild-type and *est1*Δ *ade2can1* terminal restriction fragment lengths.

Further evidence for healing by BIR came from probing for sequences that would be expected to be added from other chromosomes. A probe from chromosomes IX and X, but not XV, located just telomeric to HRII (probe B, Figure 3F), hybridized to chromosome XV in 9/23 *ade2can1* TELO colonies (Figure 3G). A probe to sequence located telomeric to HRI that is not normally present on chromosome XV (probe A, Figure 3F) hybridized to chromosome XV in 23/23 *ade2can1* TELO colonies (Figure 3H). This sequence was likely acquired by BIR since it is located distal to HRI on a number of yeast chromosomes. Neither probe hybridized to chromosome XV in control CAN^S colonies. In all of these colonies, the original chromosomes retained hybridization, indicating the translocations were nonreciprocal.

The structure of the chromosome XV rearrangements was also mapped by PCR. Primers were designed to sequences within HRI or HRII and to specific sequences present on chromosome XV or on IX and other chromosomes (Figure 3F). PCR produced the products that would be predicted if a break in chromosome XV had been healed by BIR (Figure 3I). Products from reactions using primers 5 and 2 or 6 and 4 were sequenced (data not shown), confirming that the junction between XV

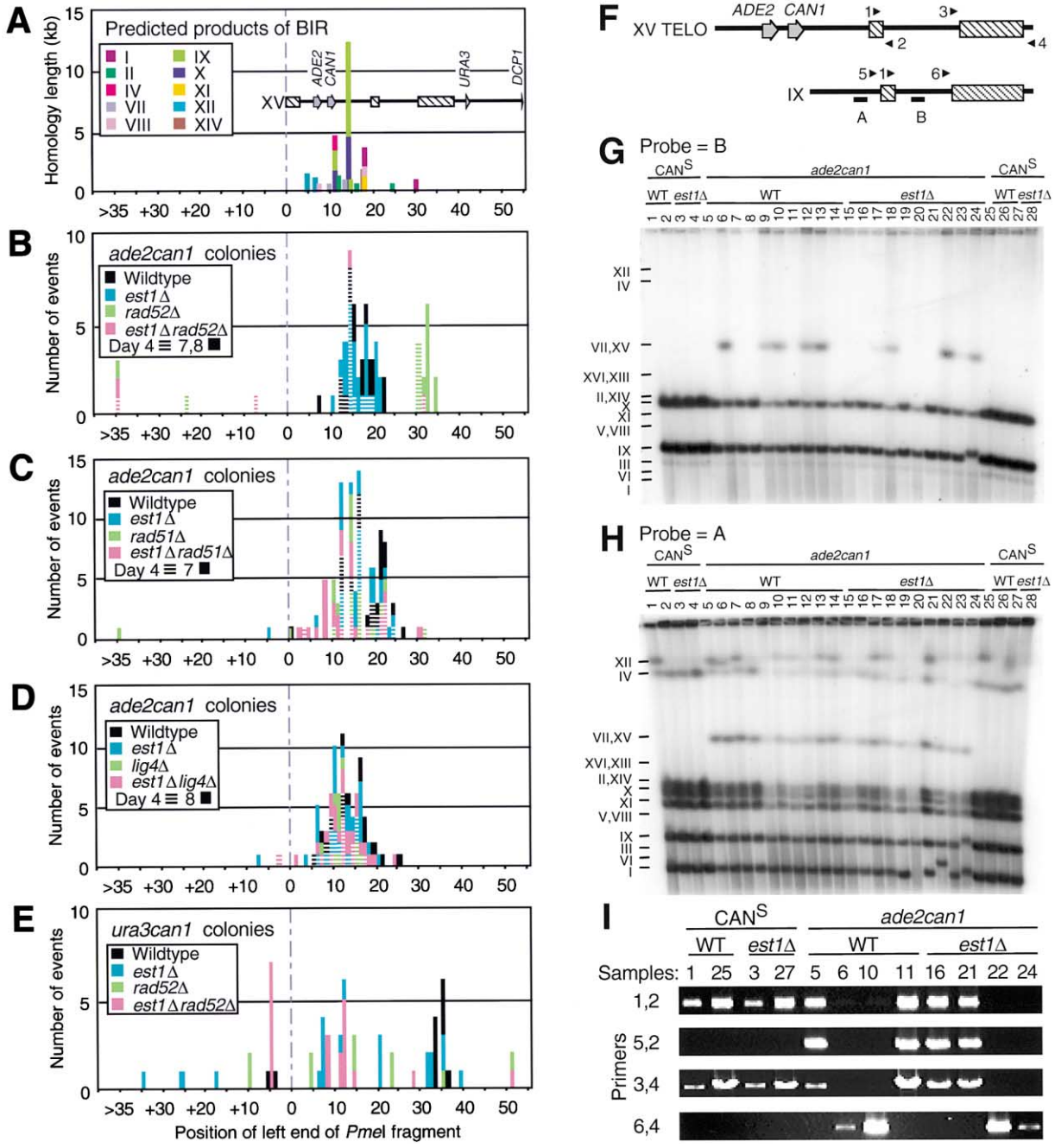

Figure 3. Analysis of Chromosome Rearrangements Recovered in the TELO Strain

(A) Position of the left end of the terminal PmeI fragment produced if BIR is used to repair a DNA break using HRI or HRII. Chromosomes with homology regions having BLAST e values $< 10^{-100}$ are shown. The length of shared homology between chromosome XV and either arm of each chromosome is indicated by the colored bars. Bars for chromosomes with the same PmeI fragment length are stacked. (B–E) The position of the left end of the PmeI fragments was estimated from the size of the band on a pulsed field gel and is indicated relative to the left telomere of chromosome XV TELO. The left end of a wild-type fragment would be located at the telomere (0 kb), while the left end of a fragment that is 10 kb shorter than wild-type would be located at 10 kb. The height of each bar represents the number of times a band of that length was observed. Bars for strains with the same PmeI fragment lengths are stacked. Hatched bars: day 4; solid bars day 7 or 8. (B) PmeI fragments from wild-type, *est1*Δ, *rad52*Δ, and *est1*Δ*rad52*Δ *ade2can1* mutant colonies. Solid bars: day 8 or 7 (*est1*Δ*rad52*Δ). Hatched bars are data from day 4. (C) PmeI fragments from wild-type, *est1*Δ, *rad51*Δ, and *est1*Δ*rad51*Δ *ade2can1* mutant colonies. (D) PmeI fragments from wild-type, *est1*Δ, *lig4*Δ, and *est1*Δ*lig4*Δ *ade2can1* mutant colonies. (E) PmeI fragments from wild-type, *est1*Δ, *rad52*Δ, and *est1*Δ*rad52*Δ *ura3can1* mutant colonies from day 7. (F) Diagram of primer sites and probe sites on chromosome XV TELO and chromosome IX used in parts (G)–(I) to identify translocations. Hatched bars represent HRI and HRII on chromosome XV TELO as shown in Figure 2A and the corresponding homology regions on chromosome IX. Telomeres are on the left. (G) Pulsed field gel of whole chromosomes probed with probe B. Chromosomes were isolated from wild-type and *est1*Δ control (CAN^S) and *ade2can1* mutant colonies. (H) Pulsed field gel of whole chromosomes probed with probe A. Samples are identical to those in (G). (I) PCR analysis of translocations. Primers are numbered in (F). DNA sample numbers correspond to those in (G) and (H). A translocation begins in HRI in samples 5, 11, 16, and 21, and begins in HRII in samples 6, 10, 22, and 24. Long-range PCR was used with primers 3,4 and 6,4.

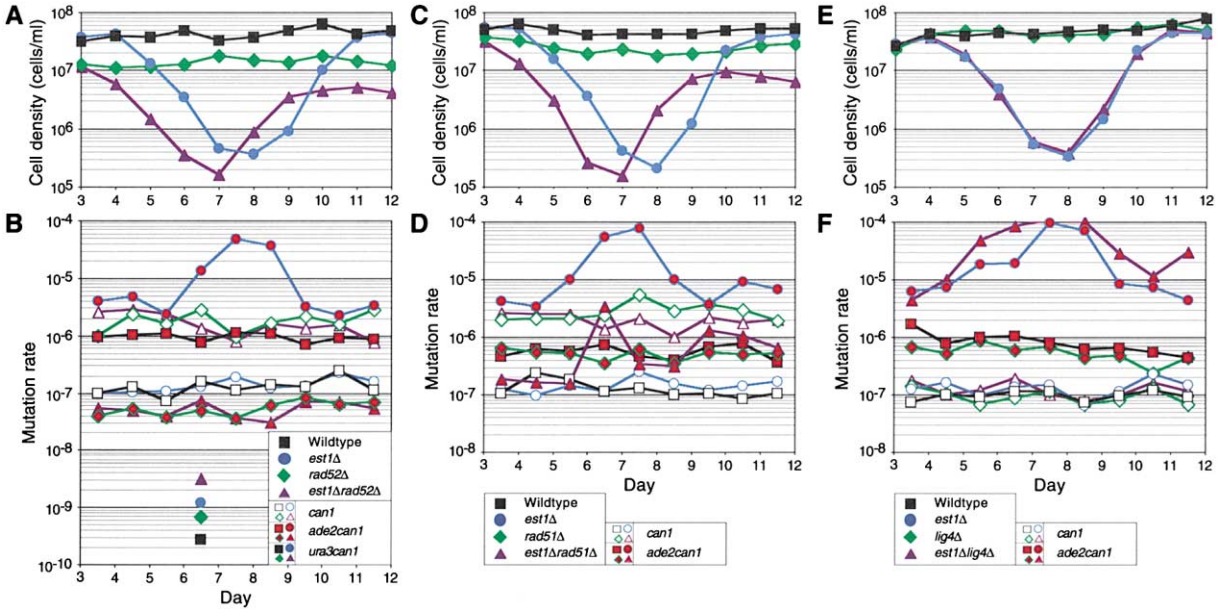

Figure 4. Effect of *rad52*, *rad51* and *lig4* on Mutation Rate in the TELO Strain

(A) Growth fraction for wild-type (black square), *est1*Δ (blue circle), *rad52*Δ (green diamond), and *est1*Δ*rad52*Δ (purple triangle) TELO strains.

(B) Mutation rate for TELO strains shown in (A). Symbols correspond to those in (A). Red centers indicate the red colony (*ade2can1*) mutation rate. White centers indicate the white colony (*can1*) mutation rate. Solid symbols at day 6.5 indicate the rate of deletion of both *URA3* and *CAN1* in the same colony.

(C) Growth fraction for wild-type (black square), *est1*Δ (blue circle), *rad51*Δ (green diamond), and *est1*Δ*rad51*Δ (purple triangle) TELO strains.

(D) Mutation rate for TELO strains shown in (C). Symbols correspond to those in (C). Red centers indicate the red colony (*ade2can1*) mutation rate. White centers indicate the white colony (*can1*) mutation rate.

(E) Growth fraction for wild-type (black square), *est1*Δ (blue circle), *lig4*Δ (green diamond), and *est1*Δ*lig4*Δ (purple triangle) TELO strains.

(F) Mutation rate for TELO strains shown in (E). Symbols correspond to those in (E). Red centers indicate the red colony (*ade2can1*) mutation rate. White centers indicate the white colony (*can1*) mutation rate.

and the other chromosome sequence was within HRI or HRII.

Rad52p-Dependent, Rad51p-Independent BIR Is Required for the Recovery of *ade2can1* Mutants in the TELO Strain

To further study the role of BIR in chromosome healing, we examined the requirement for *RAD52* and *RAD51*. BIR is dependent on Rad52p, but can occur through a Rad51p-independent pathway (Malkova et al., 1996). The increase in the red colony *CAN1* mutation rate in *est1*Δ strains, indicative of terminal deletions, was not observed in the absence of *RAD52* (Figure 4B). In fact, the *est1*Δ*rad52*Δ red colony mutation rate was indistinguishable from that of *rad52*Δ. The striking difference in the deletion rate in *est1*Δ and *est1*Δ*rad52*Δ strains suggests that RAD52p is required for either the generation or recovery, or both, of mutants with terminal deletions.

Disruption of *RAD52* should prevent the generation of *est1*Δ survivors (Lundblad and Blackburn, 1993). However, in our experiment, survivors were formed in the *est1*Δ*rad52*Δ strain (Figure 4A). Further analysis revealed that these survivors were the result of either derepression of the integrated *GAL/EST1* construct in a small number of cells, or low-level expression from this construct in some cells which might be selected when most cells arrest. Isogenic *est1*Δ*rad52*Δ strains without this integrated construct did not generate survivors (data not shown).

When *RAD51* was deleted in the *est1*Δ background, the growth rate decreased more rapidly and the culture recovered sooner, consistent with previous studies (Figure 4C) (Le et al., 1999). Overall, the red colony deletion rate was lower in the *est1*Δ*rad51*Δ strain than the *est1*Δ strain, but the rate increased when the growth rate of the *est1*Δ*rad51*Δ strain was low (Figure 4D). Therefore, Rad51p is not required for the generation or recovery of mutants with terminal deletions when telomeres are short.

To further investigate the kinds of deletions that occurred in the absence of *RAD52* or *RAD51*, we examined chromosome structure on pulsed field gels. Disruption of *RAD52* shifted the pattern of PmeI fragment lengths (Figure 3B), suggesting that *RAD52* is required for the repair of broken chromosomes by BIR. Deletion of *RAD51* did not affect the distribution of PmeI fragment lengths (Figure 3C).

Rad52p Is Not Required for the Induction of Terminal Deletions

To determine whether Rad52p had a role in the induction of terminal deletions in addition to its role in the healing of DNA breaks, we measured the *URA3CAN1* mutation rate, because BIR could not be used to heal breaks centromeric to HRII due to a lack of homology with other

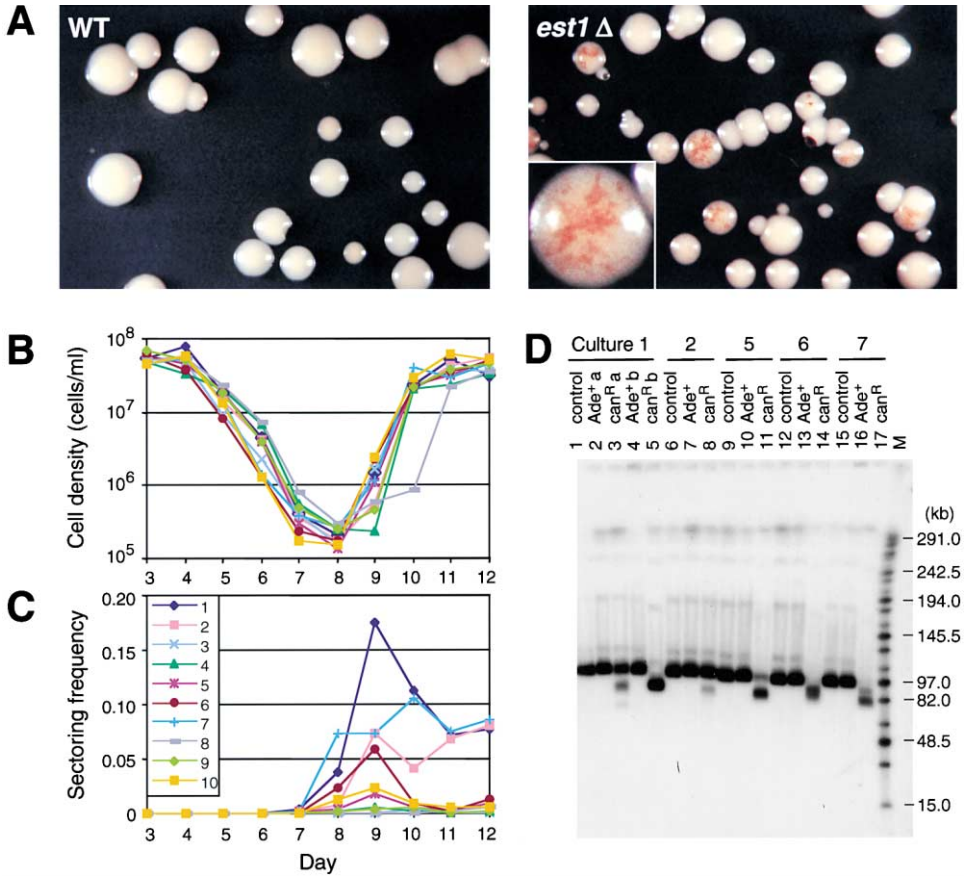

Figure 5. Sectoring of *est1*Δ Colonies

(A) Red/white sectoring late during colony growth in *est1*Δ but not wild-type TELO colonies plated on control plates.

(B) Growth rate of ten independent *est1*Δ TELO cultures. Cultures are numbered according to the legend in (C).

(C) Frequency of sectored colonies from independent *est1*Δ cultures shown in (B).

(D) Pulsed field gel of PmeI-digested DNA probed with sequence from *DCP1*. Culture numbers correspond to those in (B). Control: unsectored colony; Ade$^+$: sectored colony grown in SC-ade; can^R: sectored colony grown in canavanine. Ade$^+$ and can^R samples from the same culture are from the same colony. Two colonies (a and b) were selected from culture 1.

chromosomes (Figure 2A). Both *est1*Δ and *est1*Δ*rad52*Δ strains had *URA3CAN1* mutation rates that were nearly 10-fold higher than wild-type or *rad52*Δ (Figure 4B). Moreover, PmeI fragment lengths from *ura3can1* colonies showed no clustering according to genotype (Figure 3E). The similar increase in the *URA3CAN1* mutation rate in *est1*Δ and *est1*Δ*rad52*Δ strains suggests that Rad52p does not play a major role in the induction of DNA breaks.

Lig4p-Mediated Nonhomologous End Joining Is Not Involved in the Induction of Chromosomal Instability

To study the role of NHEJ in the generation of terminal deletions, *LIG4* (*DNL4*) was deleted. Lig4p carries out the ligation step of the main pathway of NHEJ, and it plays no known role in telomere maintenance (Teo and Jackson, 1997; Lewis and Resnick, 2000). The patterns of decreased growth and recovery were indistinguishable for the *est1*Δ*lig4*Δ and *est1*Δ strains (Figure 4E). The red colony *CAN1* mutation rate increased slightly faster in the *est1*Δ*lig4*Δ strain than in the *est1*Δ strain, but both strains had similar maximal mutation rates (Figure 4F). Deletion of *LIG4* also did not alter the pattern of recovered terminal PmeI restriction fragments (Figure 3D). These data suggest that Lig4p does not play a major role in generating or processing the gross chromosomal rearrangements in *est1*Δ TELO cells.

Ongoing Chromosomal Instability Occurs in *est1*Δ Colonies after Reintroduction of Telomerase

Colonies showing red/white sectoring that occurred late in colony growth were observed in *est1*Δ, but not wild-type TELO strains after induction of *EST1* expression (Figure 5A). The frequency of sectored colonies was quantitated in 10 independent *est1*Δ or wild-type cultures (Figure 5B). For the wild-type strain, only one sectored colony was observed among $\sim 3 \times 10^5$ colonies. However, for the *est1*Δ strain, the frequency of sectored colonies increased in each of the 10 cultures when the growth rate was low, although the magnitude of this increase varied widely between cultures (Figure 5C).

To examine the chromosomal rearrangements in the red and white sectors, cells from sectored colonies were grown in selective conditions. To isolate cells from the white sectors that retained *ADE2*, cells were inoculated into SC-ade. To isolate the cells from red sectors, cells

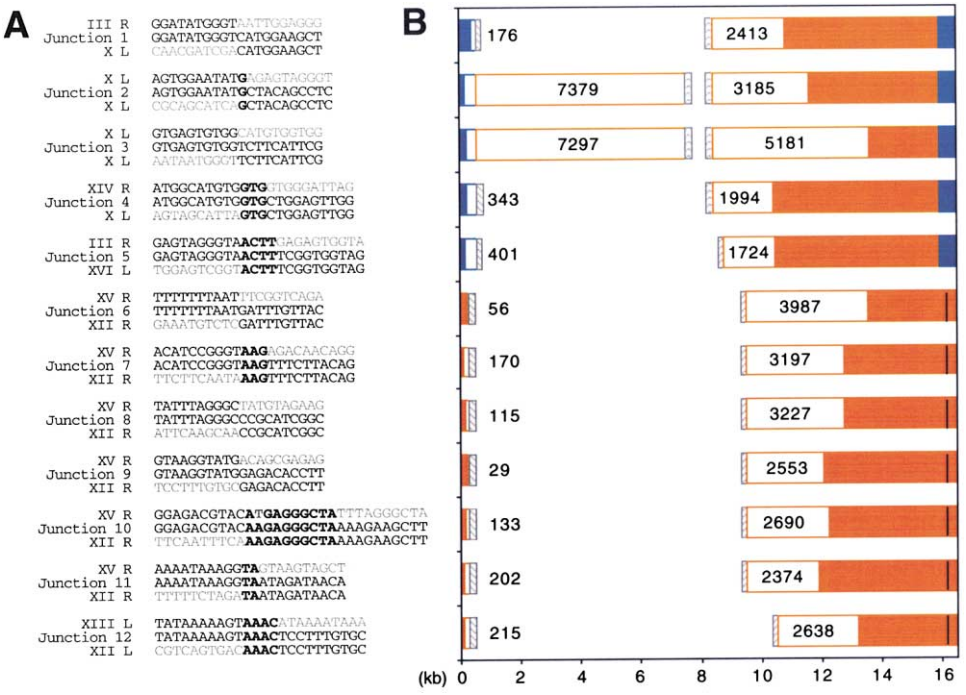

Figure 6. Isolation of End-to-End Chromosome Fusion Junctions from *est1*Δ Yeast

(A) Sequence surrounding chromosome fusion junctions amplified with a primer to the core X element (junctions 1–5) or to the Y′ element (junctions 6–12). Top and bottom lines: sequences from fused chromosomes; middle line: cloned junction sequence; bold: overlapping sequence; gray: sequence not in the clone. Because nearly identical subtelomeric sequences are often present on multiple chromosomes, only the chromosome end that has the greatest homology to the cloned sequence is indicated.

(B) Diagram of the structure of chromosome fusions. A schematic of the top chromosome is on the left and the bottom chromosome is on the right. The primer start sites are on the extreme left and right sides of the diagram. Blue: X element sequence; orange: Y′ element sequence; hatched gray: telomere repeat sequence; black line: boundary between two Y′ elements. Solid boxes are present in the cloned fusion junction. Open boxes are absent in the cloned junction fragment. The numbers inside or next to the open boxes represent the number of nontelomeric base pairs that have been lost.

were inoculated into media containing canavanine. Chromosomes from these cultures as well as from unsectored control colonies were analyzed on pulsed field gels that resolved whole chromosomes or terminal PmeI fragments. No abnormalities in *CAN1* or *DCP1* hybridization were observed in Ade$^+$ cells from sectored colonies (Figure 5D, data not shown). However, can^R cells from sectored colonies had short PmeI fragments, consistent with healing of a terminal deletion through BIR (Figure 5D). Thus, even after the restoration of *EST1* function, some *est1*Δ cultures exhibit ongoing chromosomal instability that can cause deletion of *CAN1*.

Isolation of Chromosome End-to-End Fusion Junctions from *est1*Δ Cells

The increased incidence of terminal, but not internal, deletions in *est1*Δ cells, and the ongoing chromosomal instability suggested that breakage-fusion-bridge cycles may contribute to this instability. To isolate potential chromosome fusion junctions, primers were designed to conserved sequences in subtelomeric X or Y′ elements. A single primer running 5′ to 3′ toward the telomere was used in a long-range PCR reaction. PCR products were isolated that could not be amplified from wild-type strains, but were amplified at increasing levels as telomeres shortened in *est1*Δ cells. Twelve unique chromosome fusion junctions were isolated from these reactions (Figure 6A). Interestingly, none of these junctions contained telomere sequence. All clones showed some degree of sequence loss (at least 29–7379 bp) in the X or Y′ elements before the fusion occurred (Figure 6B). Seven of these junctions contained 1–10 bp of microhomology, but five showed no apparent homology at the junction. The cloned PCR products containing junctions 1 and 6 were sequenced completely and showed no rearrangements other than the fusion junctions (data not shown). Because PCR was used to isolate these junctions, we cannot estimate how frequently chromosomes fuse. Our data indicate that end-to-end chromosome fusion occurs in *est1*Δ cultures when telomeres are short, similar to the end-to-end fusions seen in mouse metaphases with short telomeres (Blasco et al., 1997).

Discussion

To test whether telomere dysfunction leads to genetic instability that might fuel tumor progression, we assayed the mutation rate in yeast cells that show progressive telomere shortening with increased division. The mutation rate was significantly higher when the telomeres were short, and the majority of these mutant colonies contained gross terminal deletions involving nonreciprocal translocations. To observe terminal deletions in our assay, two different events must occur. First, an initiat-

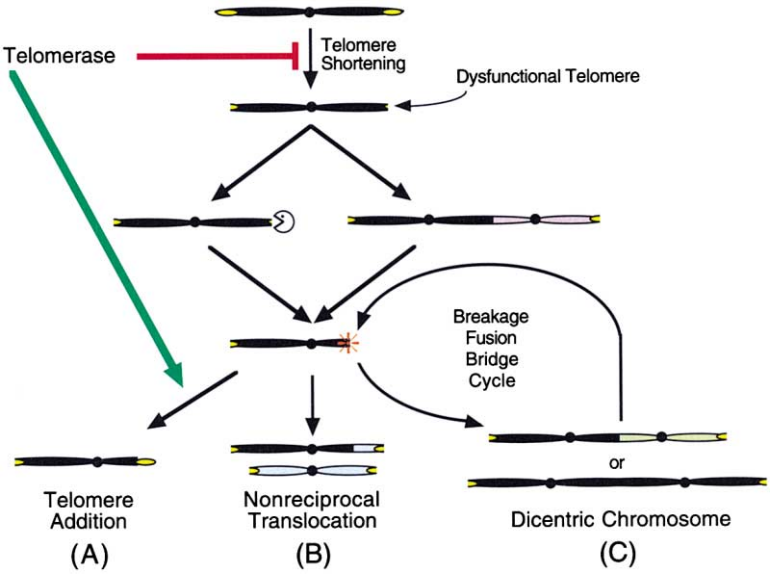

Figure 7. Model for the Role of Telomerase and Telomere Dysfunction in Chromosomal Instability

In the absence of telomerase, telomere shortening can produce dysfunctional telomeres. Dysfunctional telomeres can induce the formation of DNA breaks (orange star) through direct telomere resection, end-to-end chromosome fusion, or another mechanism. A broken chromosome can be healed by (A) de novo telomere addition, or by (B) nonreciprocal translocation through BIR or another mechanism. (C) Processing of the broken chromosome to produce a dicentric chromosome will result in subsequent DNA breaks through BFB.

ing event, such as terminal sequence loss or chromosome fusion, and second, a healing event to allow the recovery of the terminal deletion product. Below, we first discuss factors that may allow the initiation of chromosome instability, and then factors that allow recovery of the rearranged chromosome.

End-to-End Chromosome Fusion and Breakage May Initiate Terminal Deletions

Two kinds of mechanisms may be involved in the initiation of terminal deletions in cells that have lost telomere function: direct chromosome fusion leading to BFB, or terminal sequence degradation followed by BFB or directly by BIR. Chromosome fusion junctions were isolated from *est1*Δ cultures (Figure 6). The sequence at the fusion junctions and the deletion of terminal sequence are consistent with joining of chromosome ends using the error-prone pathway of nonhomologous end joining, which does not require Lig4p or Yku70p/Yku80p (Kramer et al., 1994; Boulton and Jackson, 1996; Teo and Jackson, 1997). A recent study also found a role for Lig4p-independent NHEJ in generating chromosomal rearrangements (Myung et al., 2001). Such a mechanism for the generation of chromosome fusions would explain the lack of a requirement for *RAD52* or *LIG4* in the induction of chromosomal instability (Figures 4B and 4F).

Evidence for Breakage-Fusion-Bridge Cycles

Three pieces of evidence suggest that BFB occurs in *est1*Δ strains. First, the sectored colonies in *est1*Δ strains; second, the structure of rearrangements at the native *CAN1* locus; and third, the presence of chromosome fusion junctions. The red/white sectoring of *est1*Δ TELO colonies after reactivation of *EST1* (Figure 5) indicated that there is ongoing chromosomal instability in these colonies resulting from a genomic defect that was probably present when the cells were plated. Although it is possible that the sectored colonies had lost the integrated *GAL/EST1* expression vector and were still est1$^-$, this is unlikely because the number and size of colonies was not altered, as is seen for est1$^-$ cultures. The pattern of sectoring of these colonies is consistent with the presence of BFB cycles. The absence of sectoring in the wild-type strain may be due to the absence of the initiating genomic defect.

The chromosomal rearrangements resulting from deletion of *CAN1* at the native locus frequently involved multiple chromosomes (Figures 1E and 1F). Analysis of single colonies derived from colonies with multiple *PCM1*-hybridizing bands showed that individual bands are present in different cells. This suggests that there was chromosomal instability present when the original mutant cell was plated that produced different rearrangements in different subpopulations in the colony. One mechanism by which *PCM1* could have been transferred to different chromosomes is through BFB cycles involving different chromosomes.

The isolation of end-to-end chromosome fusion junctions from *est1*Δ cultures confirms that fusions can occur. The presence of possible circular chromosomes in many *est1*Δ colonies when the native *CAN1* locus is deleted (Figure 1E) suggests that the processing of DNA breaks at some loci in *est1*Δ cells may frequently lead to chromosome fusions.

Resection of Terminal DNA May Create Terminal Deletions

If a dysfunctional telomere can no longer be distinguished from a double-strand break, it may be subject to the exonucleolytic resection that occurs at such breaks (Sugawara and Haber, 1992). Such degradation may have exposed HRI and HRII in the TELO strain, at which point BIR may have been initiated. Alternatively, terminal sequence degradation may provide the substrates for the error-prone NHEJ pathway that leads to chromosome fusions. Exonucleolytic degradation can remove at least a 34 kb stretch of chromosomal sequence (Malkova et al., 2001), and such degradation from a dysfunctional telomere is seen in *cdc13* mutants (Garvik et al., 1995).

The Mechanism and Efficiency of Repair of a DNA Break Depends on the Location of the Break and Affects the Measured Mutation Rate

The most frequent consequence of a DNA break is chromosome loss (Kramer and Haber, 1993). Because our experiments were performed in haploid strains, chromosome loss and breaks that eliminate essential genes could not be observed. The efficiency with which DNA breaks are repaired at a given locus influences the measurement of the mutation rate at that locus. There are three mechanisms that are likely involved in the restoration of a telomere to a broken chromosome: break-induced replication (BIR), de novo telomere addition, and micro- or nonhomologous translocation (Kramer and Haber, 1993; Malkova et al., 1996; Morrow et al., 1997; Chen et al., 1998).

Break-Induced Replication

BIR is the predominant pathway for healing a double-strand break if sequence near the break has homology to sequence elsewhere in the genome (Malkova et al., 1996; Bosco and Haber, 1998). The increase in the red colony *CAN1* mutation rate in the *est1*Δ TELO strain and the clustered distribution of terminal restriction fragment lengths was dependent on Rad52p, but independent of Rad51p (Figures 3 and 4), consistent with the healing of broken ends using BIR. The addition of the predicted sequence from other chromosomes to the end of chromosome XV was confirmed by hybridization of probes, PCR mapping, and sequencing (Figures 3G–3I). Thus, *CAN1* deletions in the TELO strain were associated with repair of chromosome XV by BIR.

De Novo Telomere Addition and Translocations

At the native *CAN1* locus, there are no regions of homology between *CAN1* and the first essential gene *PCM1* that might serve as substrates for BIR. Analysis of repair products when *CAN1* is deleted in strains that accumulate double-strand breaks confirms that BIR is not a predominant repair pathway at this locus (Chen and Kolodner, 1999). Instead, chromosome breaks are healed by telomere addition or micro- or non-homology-dependent translocations with similar frequencies. Recent experiments document the requirement for telomerase for the telomere addition pathway at the native CAN1 locus (Myung et al., 2001). The frequencies of rearrangements in wild-type colonies with deletions of *CAN1* in this study are consistent with these earlier studies. In 4 out of 7 wild-type colonies, deletion of *CAN1* was associated with shortening of the left arm of chromosome V to a length consistent with healing of a break between *CAN1* and *PCM1* by telomere addition (Figures 1E and 1F, data not shown). In the remaining 3 out of 7 colonies, deletion of *CAN1* was associated with interchromosomal rearrangements. No *est1*Δ colonies had fragment lengths that were consistent with de novo telomere addition, but all showed evidence of chromosomal rearrangements, many of which where more complex than those observed in wild-type colonies.

Two Roles for Telomerase in Preventing Chromosomal Instability

Telomerase likely plays two roles in chromosome stability. First, it guards against the initiation of chromosomal instability by preventing telomere dysfunction. Second, telomerase can change the spectrum, and perhaps frequency, of chromosome repair by allowing de novo telomere addition. In the absence of telomerase, a broken chromosome can either gain a telomere through a translocation event (Figure 7B) or form a dicentric chromosome that enters a BFB cycle (Figure 7C). Telomerase may prevent the initiation of a BFB cycle by allowing de novo telomere addition (Figure 7A). The separable functions of telomerase activity and telomere dysfunction in the generation of chromosomal instability may provide insight into the roles of telomeres and telomerase in tumorigenesis.

Telomerase is activated in 90% of human cancers (Kim et al., 1994). This activation stops the progressive telomere shortening that occurs in some somatic tissues and allows for unlimited cell growth. In light of this role for telomerase in tumor cell growth, telomerase inhibition was proposed as a target for inhibiting cancer cell growth. While the telomerase null mouse shows a reduction in tumor formation in some genetic backgrounds, surprisingly both the mTR$^{-/-}$ mouse and the mTR$^{-/-}$ p53$^{-/-}$ mouse show increased tumor formation (Chin et al., 1999; Rudolph et al., 1999; Artandi et al., 2000). These experiments highlighted the role of telomerase in preventing genetic instability. Our data now show directly that the absence of telomerase does increase chromosomal instability and show that telomerase can influence the structure of the resulting chromosomal changes. The kinds of chromosomal changes that we observe are similar to those observed in human tumors with loss of heterozygosity (Thiagalingam et al., 2001). They involve interchromosomal rearrangements that are initiated by DNA breaks. Moreover, the formation of dicentric chromosomes provides a mechanism whereby telomere shortening can cause both DNA breaks and chromosome gain or loss. Therefore, telomere dysfunction could be one mechanism for the initiation of chromosomal instability in tumorigenesis.

Experimental Procedures

Plasmids and Strains

To create the *GAL/EST1* expression vector (pJHU618), the genomic BamHI fragment containing *EST1* was inserted into the BamHI site in pRS403GU, which is flanked by the *GAL1* and *URA3* promoters (Nigro et al., 1992). All gene replacements and disruptions were performed using PCR-mediated gene disruption (Brachmann et al., 1998). JHUY550 (*MAT***a**/α *est1::LEU2/EST1 his3*Δ*1::*pJHU618/*his3*Δ*1 ura3*Δ*0/ura3*Δ*0 leu2*Δ*0/leu2*Δ*0 lys2*Δ*0/lys2*Δ*0*) was derived from BY4745 (Brachmann et al., 1998). One copy of *EST1* was replaced with *LEU2*, and pJHU618 was integrated into the genomic *his3*Δ*1* site.

TELO and AE Strains

TELO and AE strains were derived from a mating and sporulation of BY4705 and BY4741 (Brachmann et al., 1998) to produce the haploids (*MAT***a** *ade2*Δ*::hisG leu2*Δ*0 met15*Δ*0 ura3*Δ*0 LYS2*) and (*MAT*α *ade2*Δ*::hisG leu2*Δ*0 met15*Δ*0 ura3*Δ*0 lys2*Δ*0*). *CAN1* was replaced with *MET15* in both haploids. *CAN1*pRS402 and *URA3* were integrated into appropriate places in the genome in both haploids, as described below. pJHU618 was integrated into the *his3*Δ*1* locus of the *MAT*α haploid. The haploids were mated, and *EST1* was replaced with *LEU2*. To create *CAN1*pRS402, the genomic ApaI/BclI fragment containing *CAN1* was inserted between the ApaI and BamHI sites in pRS402. Sequences flanking the TELO *CAN1*pRS402 insertion site were amplified and cloned into *CAN1*pRS402. This vector was inserted into the genome 3482 bp from the left telomere of chromosome XV. To complete the TELO strain (JHUY635), *URA3*

was integrated between YOL155c and YOL154w. To create the AE strain (JHUY634), sequences flanking the AE *CAN1*pRS402 insertion site were amplified and cloned into *CAN1*pRS402. This vector was inserted into the genome between *SPT20* and *PEX11*. *URA3* was integrated just centromeric to *CAN1*. In the TELO strain, *RAD52* was disrupted at the BglII site by *kanMX4* to create the TELO *rad52*Δ strain (JHUY636). *RAD51* was replaced with *kanMX4* in the TELO strain to create the TELO *rad51*Δ strain (JHUY638). *LIG4* was replaced with *kanMX4* in the TELO strain to create the TELO *lig4*Δ strain (JHUY637). *lig4*Δ haploids had a 100-fold reduction in the ability to recircularize a cut plasmid, confirming the NHEJ deficiency (Teo and Jackson, 1997).

Yeast Cell Growth

Liquid growth experiments were performed in 90% minimal, 10% YEP media supplemented with 30 mg/l leucine, 30 mg/l lysine, 20 mg/l uracil, 200 mg/l ornithine (Gocke and Manney, 1979), 2% raffinose, and 0.1% dextrose. Media for TELO and AE strains was also supplemented with 87 mg/l adenine. Control plates contained 2% galactose SC-arg-his. Mutant selection plates were supplemented with 60 mg/l canavanine. Plates for measurement of the *URA3CAN1* mutation rate included 1 g/l 5-fluoroorotic acid (5-FOA) with 22 mg/l uracil. Sectored colonies were quantitated on control plates containing 32 μM adenine.

Analysis of Growth Fraction

Diploid strains were sporulated and ten independent haploid spores of each genotype were selected after 40 hr of growth (day 2). Liquid cultures were grown in log phase in 5 ml of media for 21 hr at 30°C each day. Cells were counted with a hemocytometer and diluted to a concentration (1×10^4 cells/ml for wild-type) so that cells would grow to a concentration of 2–5 $\times 10^7$ cells/ml each day to ensure enough cells for plating. 10^3 cells were plated on each control plate, and 10^8 cells or 1.5 ml were plated on each mutant selection plate. After the first 3 days of plating, 10^7 cells or 150 μl were plated on the canavanine plates for TELO *est1*Δ and *est1*Δ*lig4*Δ strains. Plates were incubated at 30°C for 3 days and the colonies were counted. To measure the *URA3CAN1* mutation rate in TELO strains, 250 ml cultures were inoculated on day 6, and the cells plated on canavanine and 5-FOA on day 7.

Mutation Rate Calculation

The number of mutants arising during the growth of the culture (R) = the total number of mutants in the culture (R_g) minus the number of mutants arising from mutant cells initially present in the culture (R_0) (Nadas et al., 1996). Therefore, $R = R_g - R_0 \times 2^g$, where g = the number of population doublings. $R_g = (mc_g \times cp_g \times N_g) / (cc_g \times mp_g)$, where mc_g = the number of mutant colonies on the selection plate; cp_g = the number of cells plated on the control plate; N_g = final number of cells in the culture; cc_g = the number of colonies on the control plate; and mp_g = the number of cells plated on the selection plate. $R_0 = (mc_0 \times N_0) / mp_0$, where mc_0 = number of mutant colonies on the previous day's selection plate; N_0 = number of cells transferred to the culture; and mp_0 = number of cells plated on the previous day's selection plate. Plating efficiency was not taken into account when calculating R_0 because it was assumed that only those mutant cells that were capable of growing into colonies would significantly contribute to the initial number of viable mutants in the new culture. This arbitrary assumption is justified empirically by the constant mutation rates in wild-type cultures. The maximal likelihood method of Lea and Coulson was used to calculate the mutation rate from the values of R (Lea and Coulson, 1949).

Colony PCR

Cells were treated with zymolyase prior to colony PCR in 96-well plates (Ling et al., 1995). The *CAN1* locus was amplified using primers JH13 (5′ GAAGAGTGGTTGCGAACAGA 3′) and JH14 (5′ GTGA GAATGCGAAATGGCGT 3′). As an internal PCR control, sequence from *CDC2* was amplified using primers JH16F (5′ CCAACCGATTT TGACCCAAG 3′) and JH16R (5′ TTCGCCTGTTTGTCGCCAAT 3′).

Pulsed Field Gel Electrophoresis

Chromosome-sized DNA was prepared in agarose plugs (Gerring et al., 1991). Gels were run in 1 × TAE at 200 V at 14°C for 26 hr with switch times of 60–120 s (whole chromosomes) or 19 hr with switch times of 1–15 s (15–300 kb). In-gel hybridization was performed with a hexamer-labeled probe (Gravel et al., 1998). Primer sequences for creating probes are available upon request.

Cloning of Chromosome Fusion Junctions

Fusion junctions were amplified using the Expand Long Template PCR system (Roche). A single primer was used in each reaction. JH60 (5′ GAATGAGATATAGATATTAAAATGTGGATAATCGTGGGC TTTATGGGTAAATGG 3′) is within the core X element. JH62 (5′ AGT ATTTCACTGTTTTGATTTAGTGTTTGTTGCACGGCAGTAGCGAGAG ACAAG 3′) is within the Y′ element. Bands were cloned into pCR-XL-TOPO (Invitrogen). Both ends of the cloned band were sequenced using M13 Forward and M13 Reverse primers.

Acknowledgments

We thank Brendan Cormack, James Haber, Forrest Spencer, and Arne IJpma for critical reading of the manuscript. We thank Jef Boeke for providing yeast strains used in this study. We thank Stephanie Smith for the cloning of *EST1*. J.H. and D.F. were supported by the Predoctoral Training Program in Human Genetics and Molecular Biology. J.H. was also supported by a National Science Foundation Graduate Research Fellowship. This work was supported by NIH grant GM43080 to C.G.

Received March 22, 2001; revised July 17, 2001.

References

Artandi, S.E., Chang, S., Lee, S.L., Alson, S., Gottlieb, G.J., Chin, L., and DePinho, R.A. (2000). Telomere dysfunction promotes non-reciprocal translocations and epithelial cancers in mice. Nature *406*, 641–645.

Blasco, M.A., Lee, H.-W., Hande, P.M., Samper, E., Lansdorp, P.M., DePinho, R.A., and Greider, C.W. (1997). Telomere shortening and tumor formation by mouse cells lacking telomerase RNA. Cell *91*, 25–34.

Bosco, G., and Haber, J.E. (1998). Chromosome break-induced DNA replication leads to non-reciprocal translocations and telomere capture. Genetics *150*, 1037–1047.

Boulton, S.J., and Jackson, S.P. (1996). Identification of a *Saccharomyces cerevisiae* Ku80 homologue: roles in DNA double strand break rejoining and in telomeric maintenance. Nucleic Acids Res. *24*, 4639–4648.

Brachmann, C.B., Davies, A., Cost, G.J., Caputo, E., Li, J., Hieter, P., and Boeke, J.D. (1998). Designer deletion strains derived from *Saccharomyces cerevisiae* S288C: a useful set of strains and plasmids for PCR-mediated gene disruption and other applications. Yeast *14*, 115–132.

Cahill, D.P., Kinzler, K.W., Vogelstein, B., and Lengauer, C. (1999). Genetic instability and darwinian selection in tumors. Trends Cell Biol. *9*, M57–M60.

Chen, C., and Kolodner, R.D. (1999). Gross chromosomal rearrangements in *Saccharomyces cerevisiae* replication and recombination defective mutants. Nat. Genet. *23*, 81–85.

Chen, C., Umezu, K., and Kolodner, R.D. (1998). Chromosomal rearrangements occur in *S. cerevisiae rfa1* mutator mutants due to mutagenic lesions processed by double-strand-break repair. Mol. Cell *2*, 9–22.

Chin, L., Artandi, S., Shen, Q., Tam, S., Lee, S.-L., Gottlieb, G., Greider, C.W., and DePinho, R.A. (1999). p53 deficiency rescues the adverse effects of telomere loss in vivo and cooperates with telomere dysfunction to accelerate carcinogenesis. Cell *97*, 527–538.

Garvik, B., Carson, M., and Hartwell, L. (1995). Single-stranded DNA arising at telomeres in *cdc13* mutants may constitute a specific signal for the *RAD9* checkpoint. Mol. Cell. Biol. *15*, 6128–6138.

Gasser, S.M. (2000). A sense of the end. Science *288*, 1377–1379.

Gerring, S.L., Connelly, C., and Hieter, P. (1991). Positional mapping

of genes by chromosome blotting and chromosome fragmentation. Methods Enzymol. *194*, 57–77.

Gocke, E., and Manney, T.R. (1979). Expression of radiation-induced mutations at the arginine permease (*CAN1*) locus in *Saccharomyces cerevisiae*. Genetics *91*, 53–66.

Gravel, S., Larrivee, M., Labrecque, P., and Wellinger, R.J. (1998). Yeast Ku as a regulator of chromosomal DNA end structure. Science *280*, 741–744.

Greider, C.W., and Blackburn, E.H. (1985). Identification of a specific telomere terminal transferase activity in *Tetrahymena* extracts. Cell *43*, 405–413.

Haber, J.E., Thorburn, P.C., and Rogers, D. (1984). Meiotic and mitotic behavior of dicentric chromosomes in *Saccharomyces cerevisiae*. Genetics *106*, 185–205.

Kim, N.W., Piatyszek, M.A., Prowse, K.R., Harley, C.B., West, M.D., Ho, P.L.C., Coviello, G.M., Wright, W.E., Weinrich, S.L., and Shay, J.W. (1994). Specific association of human telomerase activity with immortal cells and cancer. Science *266*, 2011–2014.

Kramer, K.M., Brock, J.A., Bloom, K., Moore, J.K., and Haber, J.E. (1994). Two different types of double-strand breaks in *Saccharomyces cerevisiae* are repaired by similar *RAD52*-independent, nonhomologous recombination events. Mol. Cell. Biol. *14*, 1293–1301.

Kramer, K.M., and Haber, J.E. (1993). New telomeres in yeast are initiated with a highly selected subset of TG1–3 repeats. Genes Dev. *7*, 2345–2356.

Le, S., Moore, J.K., Haber, J.E., and Greider, C.W. (1999). *RAD51* and *RAD50* define two pathways that collaborate to maintain telomeres in the absence of telomerase. Genetics *152*, 143–152.

Lea, D.E., and Coulson, C.A. (1949). The distribution of the numbers of mutants in bacterial populations. J. Genet. *49*, 264–285.

Lendvay, T.S., Morris, D.K., Sah, J., Balasubramanian, B., and Lundblad, V. (1996). Senescence mutants of *Saccharomyces cerevisiae* with a defect in telomere replication identify three additional *EST* genes. Genetics *144*, 1399–1412.

Lengauer, C., Kinzler, K.W., and Vogelstein, B. (1998). Genetic instabilities in human cancers. Nature *396*, 643–649.

Lewis, K.L., and Resnick, M.A. (2000). Tying up loose ends: nonhomologous end-joining in *Saccharomyces cerevisiae*. Mutat. Res. *451*, 71–89.

Ling, M., Merante, F., and Robinson, B.H. (1995). A rapid and reliable DNA preparation method for screening a large number of yeast clones by polymerase chain reaction. Nucleic Acids Res. *23*, 4924–4925.

Loeb, L.A. (1991). Mutator phenotype may be required for multistage carcinogenesis. Cancer Res. *51*, 3075–3079.

Lundblad, V., and Blackburn, E.H. (1993). An alternative pathway for yeast telomere maintenance rescues *est1*- senescence. Cell *73*, 347–360.

Lundblad, V., and Szostak, J.W. (1989). A mutant with a defect in telomere elongation leads to senescence in yeast. Cell *57*, 633–643.

Malkova, A., Ivanov, E.L., and Haber, J.E. (1996). Double-strand break repair in the absence of *RAD51* in yeast: a possible role for break-induced DNA replication. Proc. Natl. Acad. Sci. USA *93*, 7131–7136.

Malkova, A., Signon, L., Schaefer, C.B., Naylor, M.L., Theis, J.F., Newlon, C.S., and Haber, J.E. (2001). *RAD51*-independent break-induced replication to repair a broken chromosome depends on a distant enhancer site. Genes Dev. *15*, 1055–1060.

Marsischky, G.T., Filosi, N., Kane, M., and Kolodner, R.D. (1996). Redundancy of *Saccharomyces cerevisiae MSH3* and *MSH6* in *MSH2*-dependent mismatch repair. Genes Dev. *10*, 407–420.

McClintock, B. (1941). The stability of broken ends of chromosomes in *Zea mays*. Genetics *26*, 234–282.

McEachern, M.J., Iyer, S., Fulton, T.B., and Blackburn, E.H. (2000). Telomere fusions caused by mutating the terminal region of telomeric DNA. Proc. Natl. Acad. Sci. USA *97*, 11409–11414.

Morrow, D.M., Connelly, C., and Hieter, P. (1997). "Break copy" duplication: a model for chromosome fragment formation in *Saccharomyces cerevisiae*. Genetics *147*, 371–382.

Muller, H.J. (1938). The remaking of chromosomes. Collecting Net *13*, 181–198.

Myung, K., Chen, C., and Kolodner, R.D. (2001). Multiple pathways cooperate in the suppression of genome instability in *Saccharomyces cerevisiae*. Nature *411*, 1073–1076.

Nadas, A., Goncharova, E.I., and Rossman, T.G. (1996). Mutations and infinity: improved statistical methods for estimating spontaneous rates. Environ. Mol. Mutagen. *28*, 90–99.

Naito, T., Matsuura, A., and Ishikawa, F. (1998). Circular chromosome formation in a fission yeast mutant defective in two ATM homologues. Nat. Genet. *20*, 203–206.

Nakamura, T.M., Cooper, J.P., and Cech, T.R. (1998). Two modes of survival of fission yeast without telomerase. Science *282*, 493–496.

Nigro, J.M., Sikorski, R., Reed, S.I., and Vogelstein, B. (1992). Human p53 and *CDCHs* genes combine to inhibit the proliferation of *Saccharomyces cerevisiae*. Mol. Cell. Biol. *12*, 1357–1365.

Rudolph, K.L., Chang, S., Lee, H.-W., Blasco, M., Gottlieb, G., Greider, C.W., and DePinho, R.A. (1999). Longevity, stress response, and cancer in aging telomerase deficient mice. Cell *96*, 701–712.

Shih, I.M., Zhou, W., Goodman, S.N., Lengauer, C., Kinzler, K.W., and Vogelstein, B. (2001). Evidence that genetic instability occurs at an early stage of colorectal tumorigenesis. Cancer Res. *61*, 818–822.

Singer, M.S., and Gottschling, D.E. (1994). *TLC1*: Template RNA component of *Saccharomyces cerevisiae* telomerase. Science *266*, 404–409.

Sugawara, N., and Haber, J.E. (1992). Characterization of double-strand break-induced recombination: homology requirements and single-stranded DNA formation. Mol. Cell. Biol. *12*, 563–575.

Teo, S.-H., and Jackson, S.P. (1997). Identification of *Saccharomyces cerevisiae* DNA ligase IV: involvement in DNA double-strand break repair. EMBO J. *16*, 4788–4795.

Thiagalingam, S., Laken, S., Willson, J.K., Markowitz, S.D., Kinzler, K.W., Vogelstein, B., and Lengauer, C. (2001). Mechanisms underlying losses of heterozygosity in human colorectal cancers. Proc. Natl. Acad. Sci. USA *98*, 2698–2702.

Whelan, W.L., Gocke, E., and Manney, T.R. (1979). The *CAN1* locus of *Saccharomyces cerevisiae*: fine-structure analysis and forward mutation rates. Genetics *91*, 35–51.

Zakian, V.A. (1989). Structure and function of telomeres. Annu. Rev. Genet. *23*, 579–604.